Modeling of stress-strain state of cement-sand grouting on foundation deformation

Ludmila Strokova
Department of Geology
Tomsk Polytechnic University
Tomsk, Russia
sla@tpu.ru

Tareq Sohaib Sabah Tareq
Department of Geology
Tomsk Polytechnic University
Tomsk, Russia
sohaib85sabah@gmail.com

***Abstract* — The application of jet grouting has been becoming more widespread in the reinforcement of building foundations. This technique depends on the characteristic features of the foundation soil, relevant type of foundation and surrounding conditions. The numerical analysis was carried out with three typical load intensities, proving that the intensity of the foundation settlement being influenced by the growth of soil stiffness and strength. The calculation of vertical soil displacements is 7.9 mm before underpinning, while it is 6.5 mm after underpinning. It is defined that the use of jet structures to strengthen the ground base allows to increase the rigidity of the base and to reduce its vertical movement by 20%. The hypothetical displacements were identified of the base by varying of its mechanical properties to the optimal values.**

Keywords* — *soil, stress-strain state, reinforcement, high-pressure injection, finite element method

I. Introduction

In the last few years, designing buildings with storey erection on previous foundation excluding reinforcement is being implemented into building construction more and more. It is impossible to utilize such construction sites without specific engineering survey. In this case, the most perspective is the soil reinforcement method as this method decreases the material consumption and underpinning expenses and increases the distribution of base load-bearing capacity [1-7].

Research target: study the stress distribution behavior in subsoil and estimate the reinforcement impact on the load-bearing capacity and foundation deformation.

Administratively, studied site is located in Korostilev St, Leninsk-Kuznetsky. Geomorphologically, this area is an accumulating denuded-undulating plain. The site is located within watershed slopes adjacent to Inya River (right tributary of Ob River) valley. The studied site is within urban low-storey building area where the site surface is well-planned. North-westerly the absolute height is from 265.5 to 261.5 m. The surrounding territory is built-in area with underground water system communication.

One building within this territory is Iversk Church of Icon of the Mother of God. This rectangular-shaped building (fig. 1), dimensions in outer axis 33.28*25.78 and variable height from 4.71 to 38 m with three rounded altars. The number of storeys - two storeys with basement under the building. Maximum elevation of church: central dome - +32.0 m; built-in bell tower - +38.0 m. Building basement is girder foundation on subsoil. Foundation material involves in-situ reinforced concrete; the walls-bricks and solid reinforced concrete floor [8].

Fig. 1. View of church

II. Engineering-geological site conditions

In 2004 State Unitary Enterprise (SUE) “Kuzbassdorfondproekt” executed survey for the project planning of the Church [8]. In 2015 “Geotechnika” OOO executed survey and underpinning by reinforcement due to cracking in the foundation as a result of off-designed building extension [9].

The geological setting of this territory embraces Upper Permian sediments of the sedimentary complex overlaid by loose Quartenary sediment sequences. Upper Permian rocks include continental sediments of Ilinski subseries (P2 il) – sandstones with argillite, aleurolite and conglomerate interlayers and lenses. Quartenary eluvial sediments covered by loess loam sheath overlie eroded Upper Permian sediments.

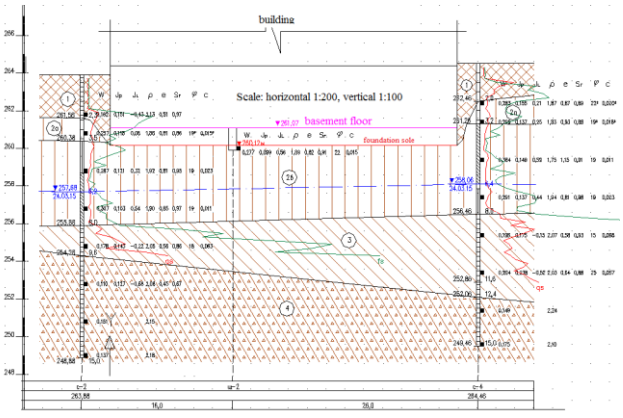

Fig. 2. Engineering-geological cross-section

Geological-lithological cross-section (fig. 2) of surveyed depth 15.0 m. (downward) includes the following engineering-geological elements (EGE):

978-1-7281-2896-2/19/$31.00 ©2019 IEEE

EGE 1(t QIV): backfilling – soil and loam composition with brick fragment inclusions of up to 20%; excavation backfill; pervasive, surficial superposed; thickness layer- 0.5-4.2m.

EGE 2 (adQIII-IV): brown loams, alluvial-deluvial; solid to high-plastic composition and saturated by iron-rich water; superposed as layers to the depth of 6.6-8.4m.

EGE 3 (adQIII-IV): clay with greyish-brown loam lenses and multi-colored eluvial solid with impurities of carbonaceous material; superposed as layers up to the depth of 9.0 – 12.5m.

EGE 4 (eQII): eluvium composition- weathering products of sandstone, argillite and siltstone; dispersed zone of crustal weathered sandstone. Soil preserves the uniform texture and structure characteristics of the parent rock, having low strength. Core sample splits and crumbles. Soil composition is heterogeneous due to different weathering rates and composition of the source material; compact in drilling; underlying penetrated layer thickness of 2.5 – 6.0 m [9].

During the survey period (March, 2015) groundwater level determined in penetrated wells was at the depth of 5.3 – 7.0 m (subsea depth 257.25 – 258.88 m).

Catchment area could be described as local and infiltrated, consequently varying according to the available precipitation, snow-melting intensity, and leakage from water systems and intervening inflow area from adjacent in-river flow.

Discharge area embraces local drainage system and fissured rocky soil and/or partially evaporates. Groundwater dynamics is non-steady, depending on climatic and technogenic conditions. Increasing level can be observed during the flood and heavy rain periods. Maximum level rise is usually in May to July, while minimum- in January-February. Seasonal groundwater fluctuation ranges from 1.0 to 1.5m in a year.

Due to the increasing high-rise building construction in 2015, underpinning was conducted by jet grouting method.

III. UNDERPINNING

Jet-grouting can also be employed as an underpinning method, as explained in [10-12]. Jet grouting is used to create one or several columns of soil-concrete under the existing structure. The advantage of this technique in underpinning is that it allows an easy access to the zone where the ground needs to be improved. Sand-cement grouting of water-cement (W/C) = 0.55-0.6 is conducted under the pressure of 0.4-0.7 MPa, through grout pipes of different lengths (4.2 and 7.2 m) to complete grout “take” during 10 minutes at predetermined pressure (fig-s 3 and 4). 4.2 m- grout pipes were used for soil foundation underpinning in basements, where 70 items were installed. 7.2m- grout pipes were used for stabilizing the soil under the external church walls and columns, where 134 items were installed. Installed grout pipes were spaced at 1 m at 5 2° vertically to the foundation axis. Grout steel pipes are of 49mm in diameter with a conical nozzle [9]. Pipe bottom (2.5m) includes a 20mm orifice every 10 cm for grouting (fig.5).

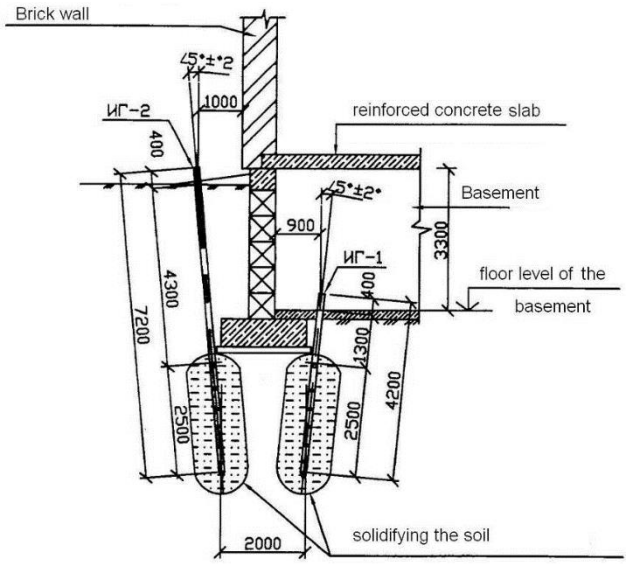

Fig. 3. Diagram of the underpinning method by jet-grouting for ground reinforcement under spread footing

Fig. 4. Execution of jet grouting in the basement

Fig. 5. Grout pipes

Grouting involves the following operations: installation of grout pipes, grouting annular space and cement-sand injection. The grouting quality is determined by check boring and core sampling throughout the operation period. Soil samples from the geotechnical mass are tested on strength and strain factors according to standard test procedure.

Construction data for underpinning is based on the test results.

IV. Modeling

The study of the solid mass stress-strain characteristics was conducted in autumn, 2016 as selected object for PLAXIS program [12]. Soil mass of 50m in length and 20m in height was presented as 2-D model. Physical-mechanical properties of soil and materials can be seen in Table 1.

TABLE I. MODEL PARAMETERS: MATERIAL PROPERTIES
Soil&Interfaces

Hardening Soil		**EGE 1**	**EGE 2**	**EGE 3**	**EGE 4**
Type		Drained	Drained	Drained	Drained
γ_{unsat}	[kN/m³]	19.00	18.40	18.40	19.80
γ_{sat}	[kN/m³]	19.00	19.00	18.90	20.80
$E50^{ref}$	[kN/m²]	50000	7000	6000	23000
$Eoed^{ref}$	[kN/m²]	97055	7000	6000	23000
power (m)	[-]	0.50	0.40	0.40	0.40
c^{ref}	[kN/m²]	1	18	11	6
φ	[°]	30	19	16	17
Eur^{ref}	[kN/m²]	300000	21000	18000	69000
ν_{ur}(nu)	[-]	0.2	0.2	0.2	0.2

Building (Plates)

ID	**Name**	**Type**	**EA**	**EI**	**w**	**ν**	**M_p**	**N_p**
			[kN/m]	[kNm²/m]	[kN/m/m]	[-]	[kNm/m]	[kN/m]
1	fund	20000	1000	3.4	0.33	1E15	1E15	1
2	fund1	50000	3000	4.0	0.33	1E15	1E15	3
3	fund-2	80000	6000	9.4	0.33	1E15	1E15	2

Basement (Anchors)

ID	**Name**	**EA**	**|F_max,comp|**	**|F_max,tens|**
		[kN/m]	[kN/m]	[kN/m]
1	Footing	2000000	1,00E+15	1,00E+15

After designing the geometrical model and determining the required soil properties, finite element mesh of 4238 irregular 15-node triangles was autogenerated in PLAXIS. In calculating the finite elements displacement is determined in the nodes, while strain- in 552 integrated Gaussian points. (or strain points).

To estimate the soil behavior the elastic-plastic model is applied with isotropic Hardening Soil Model (Plaxis). This model takes into account the differences in the elastic modulus of unloading and repeated loading distribution observed in laboratory testing experiments. The model defines exactly the soil behavior during excavation, retaining wall construction and tunneling, being followed by the average effective stress decrease and immediate mobilization of rock resistance to shearing. However, the application of above-described model is restricted due such factors as anisotropy of resistance and stiffness, creeping and fatigue strength and inadequacy for dynamic process simulation [7].

The building was designed on solid slabs supported on internode anchors. The slab specific mass is the load of the building itself [13-14]. Data describing the foundation material is assigned to the internode anchors. Initial conditions include simulated water pressure and initial strain. Calculations were integrated into the load simulation process through calculation option Staged construction.

V. RESULTS AND DISCUSSIONS

In this case, simulation determines the stress-strain changes of the soil mass under constructed building and predicting changes under conditions of underpinning by bored piles. The calculations of vertical soil thickness excluding underpinning is 9.7 mm (fig.6), while under conditions of underpinning-7.5 mm (fig. 7).

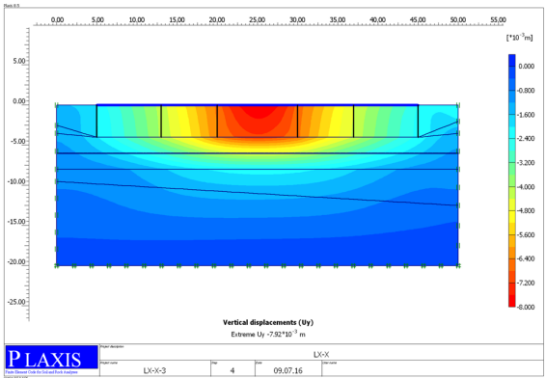

Fig. 6. Vertical displacement after building, before underpinning and grouting

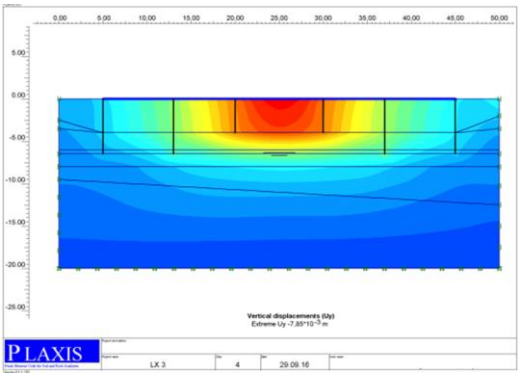

Fig. 7. Vertical displacement in soil mass after underpinning and grouting

VI. CONCLUSION

The geotechnical parameters were obtained in several in-situ tests. Based on these results the following could be stated:

- maximum settlement of the foundation depends on the load and it is observed under the central location of the building;
- increase of soil mass stiffness and strength reduces the differential settlement in the foundations;
- numerical calculation results, embracing the significant soil hererogeneity of the foundation itself, could be considered as satisfactory.

ACKNOWLEDGMENT

The research is carried out at Tomsk Polytechnic University within the framework of Tomsk Polytechnic University Competitiveness Enhancement Program grant.

REFERENCES

[1] G. G. Boldyrev and O.V. Granina, "Evaluation of the effect of reinforcement on stress-strain state of sand foundation," J. Bulletin of the Tumen University, 2003, vol.1, pp. 222-225.

[2] I. T. Mirsayapov and D.A. Artemyev, "Modeling of stress-strain state of a piled raft Foundation under combined deformation with the surrounding soil array," J. Bulletin of civil engineers, 2009, vol. 2, pp. 121-123.

[3] V. R. Mustakimov, "Experience of strengthening the foundations of buildings in the engineering-geological conditions of Tatarstan," J. Bulletin of the Kasan University. 2009, vol. 1, pp. 149-157.

[4] Y. El-Mossallamy, D. Lutz , Th. Richter, "Innovative application and design of piled raft foundation," 10th Int. Conf. on Piling and Deep Foundations, Amsterdam, 31 May - 2 June, 2006. Amsterdam, Netherlands, 2006

[5] M.F. Randolph, M.B. Jamiolkowski, and L. Zdravkovic, "Load Carrying Capacity of Foundations," Advances in Geotechnical Engineering: The Skempton Conf., ed Jardine, Potts and Higgins, 2004. pp. 207-240.

[6] O. V. Skopintseva, S.D. Ganova, N.V. Demin, and V.I. Papichev, "Integrated method of dust and gas hazard reduction in coal mines," Gornyi Zhurnal, 2018, vol. 11, pp. 97–100.

[7] A. Latypov, N. Zharkova, and A. Ter-Martirosyan, "Using plaxis software for the forecasting of karst-suffusion failures in carbonate eluvium," International Multidisciplinary Scientific GeoConference Surveying Geology and Mining Ecology Management, SGEM, 2017, vol. 17, no. 12, pp. 969-97.

[8] I. Ankudinov, "Report on geotechnical investigation of Iveron Church in Leninsk – Kuznetsk," Kemerovo, Kuzbassdorfondproekt, 2004, unpublished.

[9] V.N. Saharov, and Yu. V. Mintjanov, "Report on geotechnical investigation of Iveron Church in Leninsk – Kuznetsk", Kemerovo Geotechnika, 2015, unpublished.

[10] L.A. Strokova, Dmitrieva S.A. Osmushkina N.V., Osmushkin A.V. "Experience of engineering-geological zoning on bearing capacity of soils of the industrial site of Elga coal-preparation plant in Yakutia," Bulletin of the Tomsk Polytechnic University. Geo Assets Engineering. 2019, vol. 330, no. 2, pp. 175-185.

[11] L.A. Strokova, and E.A. Epifanova "Evaluation of deformation of a historic building in Tomsk by an Integrated Approach Based on Terrestrial Laser Scanner and Finite Element Modeling," Bulletin of the Tomsk Polytechnic University, Geo Assets Engineering. 2018. V. 329. 5. pp. 27–41.

[12] Plaxis "Material Models Manual", 2016

[13] L.A. Strokova, E.A. Epifanova, and T.G. Korzhneva "Numerical analysis of bridge foundation behaviour on the old railway line," Bulletin of the Tomsk Polytechnic University. Geo Assets Engineering, 2017, vol. 328, no. 5, pp. 125–139.

[14] J.H. Boushehrian, and N. Hataf, "Experimental and numerical investigation of the bearing capacity of model circular and ring footings on reinforced sand," Geotextiles and Geomembranes. 2003, vol. 21, no. 4, pp. 241–256.